X-ray magnetic circular dichroism study of spin reorientation transitions of magnetic thin films induced by surface chemisorption

Daiju Matsumura, Toshihiko Yokoyama,* Kenta Amemiya, Soichiro Kitagawa, and Toshiaki Ohta
Department of Chemistry, Graduate School of Science, The University of Tokyo, 7-3-1 Hongo, Bunkyo-ku, Tokyo 113-0033, Japan
(Received 12 February 2002; published 24 June 2002)

Spin reorientation transitions of Co and Ni thin films induced by surface chemisorption have been investigated for CO-adsorbed Co/Pd(111) and CO- and H-adsorbed Ni/Cu(001) by means of Co $L_{III,II}$- and Ni $L_{III,II}$-edge x-ray magnetic circular dichroism (XMCD). For four to six monolayer (ML) Co/Pd(111), a spin reorientation transition from surface parallel to perpendicular magnetization has been observed at 200 K after CO dosage. The region of perpendicular magnetic anisotropy (PMA) becomes about 3 ML thicker at this temperature. For Ni/Cu(001), similar transitions have been confirmed when the layers are covered with CO or H, and the PMA range is also expanded, in this case by about 2 ML. The observed stabilization of perpendicular magnetic anisotropy due to chemisorption is ascribed to quenching of the surface parallel magnetic orbital moment. The effects of the fashion in which adsorption occurs on the easy axis of thin-film magnetization are also examined by comparing the differences in behavior between CO- and H-adsorbed Ni films.

DOI: 10.1103/PhysRevB.66.024402 PACS number(s): 75.70.Ak, 87.64.Ni, 61.10.Ht

I. INTRODUCTION

The magnetic anisotropy of ultrathin films has been studied widely by many researchers in recent decades. The direction of the easy axis of magnetic films is influenced by the existence of surface, interface, and elastic strains for epitaxial growth. Especially, thin Co layers sandwiched between nonmagnetic metals such as Pd, Pt, and Au are well known to exhibit strong perpendicular magnetic anisotropy (PMA).[1–5] Below the critical thickness, typically five to ten monolayers (ML), Co layers show a perpendicular magnetic easy axis, which would be energetically unstable if one considers only classical magnetic dipole-dipole interaction. Numerous studies, both experimental and theoretical, have revealed that the origin of the perpendicular easy axis is directly related to the interface anisotropy.[2] Since Co single-layer films show weaker PMA than sandwiched multilayer films,[6] it is reasonable to assume that PMA is stabilized at the interface between Co and the nonmagnetic spacers. X-ray magnetic circular dichroism (XMCD) experiments[2,7] have indicated large perpendicular orbital moments in Co multilayer films compared to that in bulk Co and have concluded that strong anisotropy of orbital moments stabilizes PMA. Another experimental study using the standing-wave method has clarified that the orbital moment is actually enhanced in the vicinity of the interface between Co and the substrate,[8] a finding that is consistent with theoretical predictions.[9,10]

The effect of surface chemisorption on the magnetic easy axis is also an interesting subject. It has been revealed by means of the magneto-optical Kerr effect[11,12] (MOKE) that the PMA of the Ni/Cu(001) system[13] is stabilized when it is covered with CO or H. Slightly below the critical thickness, a spin reorientation transition was observed from the surface parallel to the perpendicular direction. It was concluded, phenomelogically, that the contribution of surface anisotropy, which favors parallel magnetization, is significantly reduced due to the interaction between surface Ni and the adsorbates. Other examples of the rotation of the easy axis induced by gas adsorption have been reported in systems such as CO/Co/Pt(111) (Ref. 14), CO/Co/Cu(110) (Refs. 15 and 16), CO,H,O/Fe/W(110) (Ref. 17), and O/Fe/Ag(001) (Ref. 18). H/Fe/Cu(001) also shows the spin reorientation transition induced by H adsorption,[19] although in this case H adsorption results in the structural transformation of the Fe film itself and the change in surface anisotropy might be a minor effect. In order to elucidate the origin of the mechanism of these spin reorientation transitions from a microscopic viewpoint, it is necessary to first understand the orbital magnetic moment that determines the magnetic easy axis. For this purpose, the XMCD technique is one of the most suitable methods, as in the case of PMA in a sandwiched Co multilayer film.

In the present study, we have investigated the effect of chemisorption on the magnetic easy axis of Co/Pd(111) and Ni/Cu(001) by means of XMCD. As a source of chemisorbed gases, we have employed CO for both films and H for Ni/Cu(001). CO is one of the most popular chemisorption gases. It adsorbs atop sites as well as bridge sites of Co and Ni surfaces with the molecular axis perpendicular to the surface. It is known that CO adsorption reduces the magnetization of the films. In addition, we observed an induced magnetic moment in CO adsorbed on Ni and Co films.[20–22] H adsorption is also interesting, because H adsorbs at the fourfold hollow site on Ni(001) (Ref. 23) and the fashion by which it adsorbs, being different from that of CO, may lead to a different mechanism underlying the transition. In this work, we have discovered a spin reorientation transition of Co/Pd(111) after CO adsorption at 200 K. In the case of CO- and H-adsorbed Ni/Cu(001), the spin reorientation transitions were confirmed as observed in the previous works.[11,12] Here we reveal the correlation between adsorbates and surface magnetism from the observed spin and orbital magnetic moments in order to obtain a more precise understanding on the magnetic anisotropy of metal thin films.

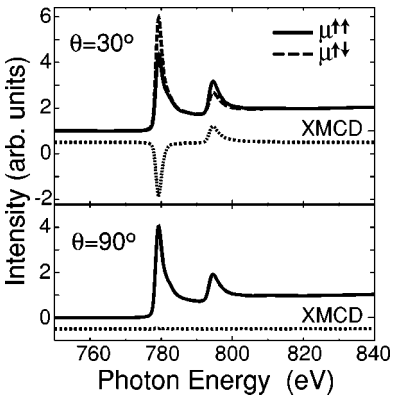

FIG. 1. Co $L_{\mathrm{III,II}}$-edge circularly polarized and XMCD spectra of a clean 4.5-ML Co film on Pd(111) taken at 200 K and x-ray incident angles of θ=30° (grazing) and θ=90° (normal).

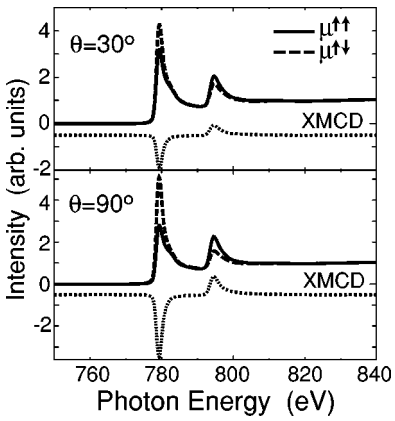

FIG. 2. Co $L_{\mathrm{III,II}}$-edge circularly polarized and XMCD spectra of a CO-adsorbed 4.5-ML Co film on Pd(111) taken at 200 K and x-ray incident angles of θ=30° (grazing) and θ=90° (normal).

II. EXPERIMENTS

Co thin films were prepared on a Pd(111) single crystal by the following procedure. The Pd(111) substrate was cleaned by repeated cycles of Ar^+ sputtering (2 keV) and annealing at ~1070 K in an ultrahigh-vacuum chamber. Sample annealing was performed by electron bombardment from the rear side of the crystal, and the temperature was monitored with a Chromel-Alumel thermocouple. The cleanliness and order of the surface were confirmed by NEXAFS (near-edge x-ray-absorption fine structure), AES (Auger electron spectroscopy), LEED (low-energy electron diffraction), and RHEED (reflection high-energy electron diffraction). The Co thin films were deposited on Pd(111) at room temperature with the electron-beam evaporation method. The thickness of the films was calibrated by the AES intensity ratio between Co and Pd. The Ni thin films were prepared on Cu(001) in a similar manner. The Cu(001) substrate was cleaned by Ar^+ sputtering (1.5 keV) and annealing at ~900 K. The Ni thin films were deposited at room temperature by evaporation from a resistively heated wire. The thicknesses of the films were calibrated by *in situ* observation of the RHEED oscillations. The samples were dosed with appropriate amounts of CO or H_2 at 200 K (CO/Co/Pd, H/Ni/Cu) or 300 K (CO/Co/Pd, CO/Ni/Cu). The temperature of 200 K was obtained by using an ethanol slurry.

The Co $L_{\mathrm{III,II}}$- and Ni $L_{\mathrm{III,II}}$-edge XMCD spectra were taken at the bending-magnet station Beamline 7A of the Photon Factory at the Institute of Materials Structure Science, High Energy Accelerator Research Organization (KEK-PF).[24] Circularly polarized x rays were obtained by using the upper (0.4 ± 0.1 mrad, positive helicity) or lower (-0.4 ± 0.1 mrad, negative helicity) part from the synchrotron orbit plane. The circular polarization factor was estimated to be $P_c=0.80$ by measuring the Co $L_{\mathrm{III,II}}$- and Ni $L_{\mathrm{III,II}}$-edge XMCD spectra of bulk Co and Ni prepared *in situ*. All the spectra were recorded in a partial-electron-yield mode using a detector consisting of a 25-mm-diam microchannel plate (MCP) and two Au-coated W grids; this detector was placed below the sample. To enhance the surface-to-bulk ratio of the signals, the solid angle was limited so that it would collect electrons with grazing emission only. Retarding voltages (-500 and -600 V for Co and Ni L edges, respectively) were applied to the second grid (closer to the MCP), while the first one was grounded. The intensity of the incident x rays (I_0) was monitored simultaneously with an Au-coated W mesh placed in the upstream of the sample.

The XMCD spectra were obtained by reversing the magnetization of the films or the helicity of the incident x rays. Each sample was mounted in a Helmholtz coil and was magnetized by a current pulse (~0.1 T) along the incident x rays. The remanent magnetization was examined. For the detection of magnetization, XMCD measurements were performed at grazing x-ray incidence (θ=30°) and normal incidence (θ=90°) angles. Here θ is the x-ray incident angle between the electric field vector of x rays and the surface normal.

III. RESULTS

A. CO on Co/Pd(111)

Figure 1 shows the Co $L_{\mathrm{III,II}}$-edge spectra with circularly polarized x rays and the XMCD spectra of a clean 4.5-ML Co film grown on Pd(111) taken at 200 K. The circularly polarized spectra $\mu^{\uparrow\uparrow}$ and $\mu^{\uparrow\downarrow}$ were obtained by dividing the partial-electron-yield spectra with the I_0 function measured simultaneously, subsequent pre-edge linear background subtraction, normalization with the edge jumps, and consequent correction of the self-absorption effect.[25] Here $\mu^{\uparrow\uparrow}$ and $\mu^{\uparrow\downarrow}$ correspond to the spectra with the photon helicity parallel and antiparallel, respectively, to the majority spin of the sample. XMCD is defined as the difference between $\mu^{\uparrow\uparrow}$ and $\mu^{\uparrow\downarrow}$, normalized with the factor of P_c. As indicated in Fig. 1, the easy axis of the films lies parallel to the surface and no XMCD signal is observed at normal x-ray incidence. By dosing the Co film with saturated amounts of CO [~4 L (1 L=10^{-6} Torr s, 1 Torr=133 Pa)] at 200 K, the spectra have changed drastically, as shown in Fig. 2. The XMCD signal appears at normal x-ray incidence, implying the occurrence of a spin reorientation magnetic phase transition by CO adsorption.

Our quantitative evaluation uses the well-established XMCD sum rule for the L edge.[26,27] The $3d$ hole numbers in

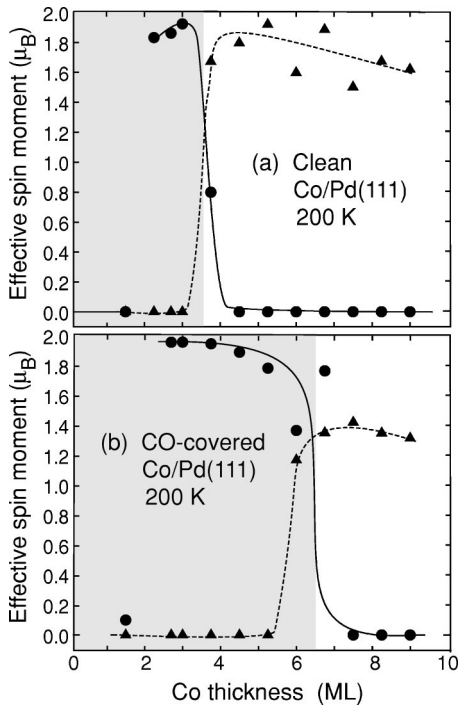

FIG. 3. Effective spin magnetic moments of (a) clean and (b) CO-covered Co films on Pd(111) at 200 K as a function of Co thickness. Circles and solid lines correspond to the surface normal direction, while triangles and dashed lines correspond to the surface parallel one. Hatched areas indicate the PMA regions.

the present Co and Ni thin films were obtained by comparing the white-line intensities with the bulk ones and using the $3d$ hole numbers in bulk Co and Ni of 2.5 and 1.4 (Ref. 28), respectively. Since the magnetic dipole term $\langle T_z \rangle$ in the spin sum rule was not taken into account, the obtained spin magnetic moment is effective ($m_s^{eff}=m_s+7\langle T_z \rangle$). Figure 3(a) shows the effective spin magnetic moments of Co/Pd(111) at 200 K with various Co thicknesses for the surface normal and parallel directions. Below ~3 ML, the film shows perpendicular magnetization, while above ~4 ML the film exhibits surface parallel magnetization. Thus, the critical thickness is ~3.5 ML, the same as it was for 300 K in the previous report.[6] The 1.5-ML Co film shows no magnetization in either direction, implying a Curie temperature below 200 K.

In the case shown in Figs. 1 and 2, the 4.5-ML Co film gives inherently a parallel magnetic easy axis and undergoes a spin reorientation transition from the in-plane to perpendicular direction upon CO adsorption at 200 K. The effective spin magnetic moments are plotted in Fig. 3(b) as a function of Co thickness. One can see that films thinner than ~6.5 ML exhibit PMA. The critical thickness increases by ~3 ML compared to that of clean surface films (~3.5 ML) in Fig. 3(a). On the other hand, no shifts in the critical thickness were observed for CO adsorption at 300 K. Figure 4 shows the effective spin moment along the surface normal direction for both clean and CO-covered Co/Pd(111) at 300 K. Here, the amount of CO dosage was also 4 L, and we confirmed that the CO coverage is saturated completely. The decrease in the spin magnetic moment from 3 ML to 1

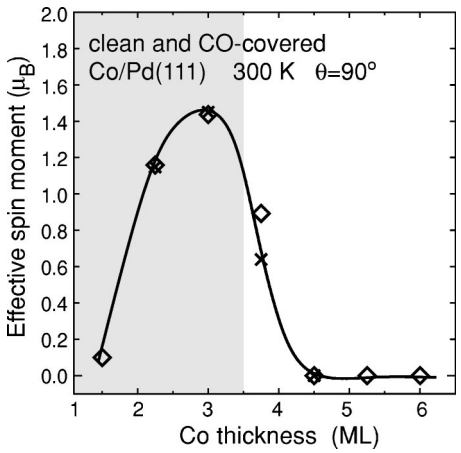

FIG. 4. Effective spin magnetic moments along the surface normal direction for clean (diamond) and CO-covered (cross) Co films on Pd(111) at 300 K as a function of Co thickness. The hatched areas indicate the PMA region.

ML Co originates in the temperature effect, and PMA was confirmed to be in the range thinner than <3.5 ML. Although there are fewer data points than there were at 200 K, it is worth noting that the critical thickness of ~3.5 ML is not affected by the adsorption of the saturated amount of CO.

B. CO and H on Ni/Cu(001)

Figures 5 and 6 show the XMCD spectra of CO-adsorbed and H-adsorbed Ni/Cu(001). The clean Ni/Cu(001) films exhibit in-plane magnetization, because a strong XMCD signal was observed for the grazing-incidence (θ=30°) data, while no signals were detected for normal incidence (θ=90°). After adsorption of saturated amounts of CO (300 K) or H (200 K), the XMCD signals at normal incidence are dominant in both Figs. 5 and 6, clearly implying the occurrence of the spin reorientation transition induced by gas adsorption. In the case of H adsorption, it was also found in Fig. 6 that when the H-covered Ni film is annealed to ~300 K, the adsorbed hydrogen desorbs and the in-plane magnetization is, for the most part, recovered.

Figure 7 shows the effective spin moment of Ni/Cu(001) as a function of CO coverage. The effective spin moment

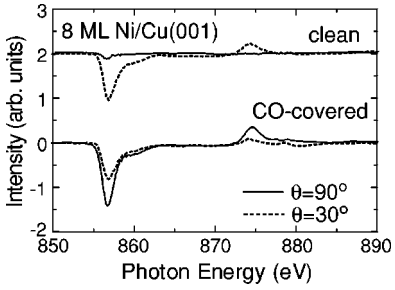

FIG. 5. Ni $L_{III,II}$-edge XMCD spectra of the clean and CO-adsorbed 8 ML Ni film on Cu(001) taken at 300 K. Solid lines correspond to the normal x-ray incidence spectra (θ=90°), and dashed lines correspond to the grazing x-ray incidence ones (θ=30°).

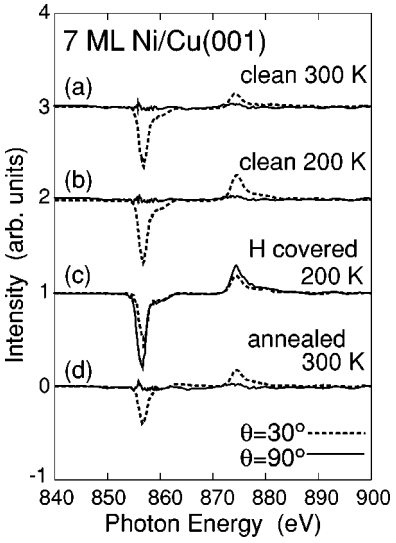

FIG. 6. Ni $L_{\mathrm{III,II}}$-edge XMCD spectra of 7-ML Ni film on Cu(001): (a) the initially prepared clean Ni at 300 K, (b) after subsequent cooling to 200 K, (c) after H adsorption at 200 K, and (d) after annealing H-covered Ni to 300 K. Solid lines correspond to the normal x-ray incidence spectra (θ=90°), and dashed lines correspond to the grazing x-ray incidence ones (θ=30°).

was obtained in a manner similar to that in the above Co/Pd(111) case. Unlike the case of Co, Ni films thinner than ~9.5 ML show in-plane magnetization, while thicker films exhibit PMA. Upon CO adsorption, the critical thickness becomes ~7.5 ML, which is ~2 ML thinner than that in clean Ni/Cu(001). These results are consistent with the previous reports.[11,12] Figure 7 also shows that the remanent magnetization increases with the Ni thickness. This, again, originates from the difference in reduced temperature in Ni thin films.

C. Orbital magnetic moment

To provide a more detailed understanding of the spin reorientation transition, Fig. 8 shows changes in the orbital magnetic moments in Co/Pd(111) induced by CO exposure at 200 K. From the viewpoint of the magnetic easy axis, we can

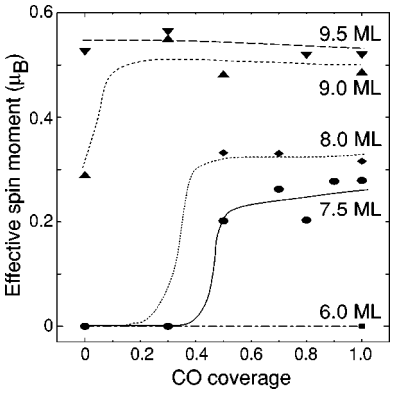

FIG. 7. Effective spin magnetic moments along the surface normal direction of the Ni films on Cu(001) at 300 K as a function of CO coverage. Here, the saturated adsorption is assumed to be a unit CO coverage.

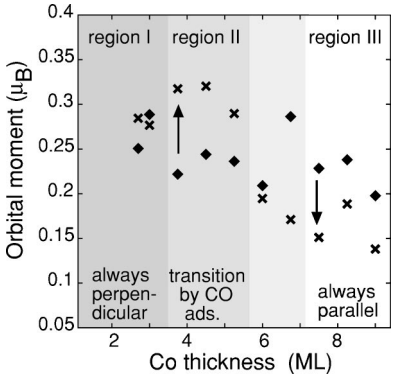

FIG. 8. Orbital magnetic moments of the Co films on Pd(111) at 200 K as a function of Co thickness. Diamonds and crosses denote clean and CO-adsorbed Co, respectively. Note that there exists a mixture phase between regions II and III, where the perpendicular or parallel orbital moment is poorly defined.

classify Co thickness into three regions. Below 3 ML, Co films show perpendicular magnetization even before CO adsorption (region I). Above 7 ML, on the other hand, Co films show parallel magnetization even after CO adsorption (region III). In the thickness range between 3 and 7 ML, Co films exhibit the spin reorientation transition (region II). As seen in region I, the perpendicular orbital magnetic moments are left unchanged upon CO adsorption. In region II, the orbital magnetic moment after CO adsorption (perpendicular magnetization) is greater than that before CO adsorption (parallel). In region III, adsorption of CO causes reduction of the parallel orbital magnetic moments. A similar change with the Co thickness is also observed in the ratio of the orbital/spin magnetic moments, although no corresponding figures are shown.

In the case of Ni/Cu(001), it is hard to compare the absolute values of the orbital moments in the thin films with each other, because they depend on the Curie temperature. Instead, we use the ratio of the orbital/spin moments. The ratio for 8 ML Ni/Cu(001) is obtained as 0.27 ± 0.03 for clean (parallel magnetization), 0.23 ± 0.03 for CO-adsorbed (perpendicular), and 0.16 ± 0.03 for H-adsorbed Ni (perpendicular), respectively. The CO-adsorbed film gives nearly the same value as the clean one within a margin of error. On the other hand, in the H-adsorbed film, the ratio is much smaller than in the clean film. Although both of these results imply suppression of the orbital moments parallel to the surface by gas adsorption, a different mechanism in the spin reorientation transitions should be proposed because of the different behaviors in the orbital/spin moment ratios. In the case of 4.5 ML Co/Pd(111), the orbital/spin moment ratio is given as 0.13 ± 0.01 for clean (parallel) and 0.17 ± 0.01 for the CO-adsorbed (perpendicular) film, respectively. The ratio is found to increase, which is, again, in clear contrast to the case with CO/Ni/Cu(001).

IV. DISCUSSION

Magnetic anisotropy of thin films is governed by magnetoelastic, magnetocrystalline, and shape anisotropies. Shape

anisotropy always favors parallel magnetization because of classical magnetic dipole-dipole interaction. Magnetoelastic anisotropy is induced by pseudomorphic growth on the substrate, while magnetocrystalline anisotropy is mainly caused at the surface and interface, where the interatomic potential should be different from that in the bulk. Here, the bulk contribution in magnetocrystalline anisotropy is neglected because the present films grow on the fcc substrates with cubic symmetry and we discuss here differences in magnetization between the in-plane and perpendicular directions. The direction of the easy axis of thin films is described by the second-order magnetization anisotropy energy. This is given by the sum of volume (K_{2v}), surface (K_{2s}), and interface (K_{2i}) anisotropy energies,

$$\Delta E = -2\pi M_{sat}^2 + K_{2v} + (K_{2s} + K_{2i})/d, \tag{1}$$

where M_{sat} is the saturated magnetization that corresponds to shape anisotropy and d is the thickness of the film. K_{2v} is ascribed to magnetoelastic anisotropy and K_{2s} and K_{2i} to magnetocrystalline anisotropies at the surface and interfaces, respectively. If ΔE is positive, perpendicular magnetization is favored.

For Ni/Cu(001), the magnetoelastic anisotropy constant K_{2v} is positive due to the pseudomorphic growth,[13,29] while both surface and interface anisotropy constants (K_{2s} and K_{2i}) are negative. These competing anisotropies make the Ni films perpendicularly magnetized only at thicknesses above ~10 ML, where the contribution of the surface and interface is relatively small. For Co/Pd(111), on the other hand, since interface magnetocrystalline anisotropy is the essence of PMA, a perpendicular easy axis appears below the critical thickness. A large perpendicular orbital moment ($0.26\mu_B$) reported by a previous XMCD experiment[2] implies the stabilization of PMA.

Let us discuss the quenching mechanism of the orbital magnetic moments in the surface parallel direction upon chemisorption. When the parallel orbital moment of the surface atoms is reduced, surface anisotropy is suppressed, leading to the stabilization of PMA. Schematic pictures of the orbital moments of the surface atoms are depicted in Fig. 9. As long as CO adsorbs on the atop site, the perpendicular orbital moment, which is derived from in-plane orbitals, is barely quenched. On the other hand, out-of-plane electron orbitals, which induce the parallel orbital moment, interact with CO strongly, leading to significant quenching of the in-plane orbital moment. This picture can be applied to both the CO-adsorbed Co/Pd(111) and Ni/Cu(001) films. In CO/Co/Pd(111), this effect causes almost no change in the perpendicular orbital moment in region I, but significant suppression of the parallel orbital moment by CO reduces the absolute value of K_{2s}, leading to the stabilization of PMA.

In the case of H adsorption on Ni/Cu(001), a more significant decrease in the orbital moment is observed compared to the case of CO/Ni/Cu(001). As mentioned above, the orbital/spin magnetic moment ratio was 0.27 ± 0.03 for clean (parallel magnetization), 0.23 ± 0.03 for CO-adsorbed (perpendicular), and 0.16 ± 0.03 for H-adsorbed Ni (perpendicular). H adsorbs at the fourfold hollow site[23] and significantly

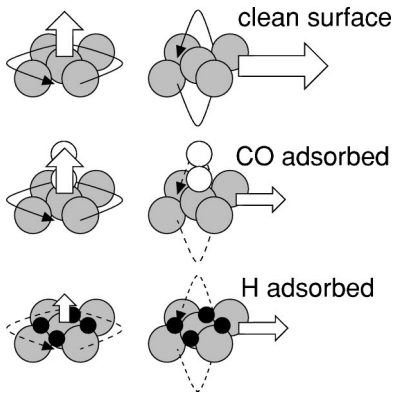

FIG. 9. Schematic pictures of the orbital moments of surface atoms. Rotating arrows (thin solid and thin dashed lines) indicate the rotation of the $3d$ electrons, and straight arrows indicate corresponding angular momenta. A parallel orbital moment is always favored over a perpendicular one for the atoms in the topmost layer of the clean surface. Note that here only those atoms are considered. Upon CO adsorption, the perpendicular orbital moment, which originates from the electron rotation in the surface plane, is almost unchanged because the CO molecules are standing up at the atop site, while the parallel orbital moment due to the out-of-plane rotation of the electrons is significantly quenched because of the hindrance of CO at the surface. In the case of H adsorption, both the perpendicular and parallel orbital moments are noticeably quenched because of the fourfold hollow site adsorption. Although the (001) surfaces are assumed in this figure, a similar mechanism can be applied to CO/Co/Pd(111).

reduces the orbital magnetic moments in both the parallel and perpendicular directions, as explained in Fig. 9. This is in striking contrast to the case of CO adsorption, in which the suppression of the perpendicular orbital moment is not so important. The difference in the perpendicular orbital/spin ratios between CO/Ni and H/Ni can thus be explained. Although PMA is resultantly stabilized in both CO and H adsorption, different microscopic mechanisms are proposed for the spin reorientation transitions.

As for the structure of metal thin films, 9% of the lattice mismatch exists in Co/Pd(111). Although nonpseudomorphic growth was observed by means of RHEED,[6] the EXAFS (extended x-ray-absorption fine structure) study[30] indicated the presence of the strain originating from the lattice mismatch in films of a few ML. The structure of the Co films on Pd(111) is not well understood. Since magnetoelastic anisotropy induced by pseudomorphic growth is the key to PMA for Ni/Cu(001), it should also be important to consider the structure of the Co thin film. Intermixing at the interface is another possibility to explain magnetic anisotropy, because a recent experiment pointed out the formation of alloy structure in the Co/Pd interface.[31] In this study, we cannot discuss the effects of film structures on magnetic anisotropy. However, since the surface tension of the film would relax in a few ML, we can rule out the possibility of structural change of the films for determining the easy axis of the Co thin films. The complexity of the structure at the interface does not allow us to distinguish between magnetoelastic and magnetocrystalline anisotropies. Furthermore, it is difficult to un-

derstand why the shift in the critical thickness is not observed at 300 K in the case of CO/Co/Pd(111). The possibility of a different CO adsorption site on the surface cannot be ruled out. For CO adsorption on hcp Co(0001), it has been reported that CO adsorbs on both atop and bridge sites at 180 K.[32] Theoretical calculations have predicted differences in magnetic interactions at different adsorption sites.[33] The adsorption site of CO on the present Co/Pd(111) films has not been determined yet. These microscopic explanations of surface and interface magnetic states may thus be a subject of future studies.

V. CONCLUSIONS

We investigated the effects of adsorption on the magnetic easy axis in Co/Pd(111) and Ni/Cu(001) by using XMCD. We found that PMA is stabilized by adsorption of CO on Co/Pd(111) at 200 K and that the critical thickness increased by about 3 ML. A similar PMA stabilization was confirmed for Ni/Cu(001) by adsorption of CO and H. From the change of orbital moments from before to after chemisorption, the stabilization of PMA by CO is attributed to the reduction of surface parallel magnetic orbital moment. The PMA stabilization induced by H is concluded to originate from a different mechanism, which in turn is attributed to the different adsorption fashion of H.

ACKNOWLEDGMENTS

The authors gratefully acknowledge Yasuhiro Hamada and Norihiro Suzuki for their support in the experiments and data analysis. The present work has been performed under the approval of the Photon Factory Program Advisory Committee (PF-PAC No. 99G159).

*Present address: Institute for Molecular Science, Myodaiji-cho, Okazaki, Aichi 444-8585, Japan. Electronic address: yokoyama@ims.ac.jp

[1] Y. Wu, J. Stöhr, B. D. Hermsmeier, M. G. Samant, and D. Weller, Phys. Rev. Lett. **69**, 2307 (1992).
[2] D. Weller, Y. Wu, J. Stöhr, M. G. Samant, B. D. Hermsmeier, and C. Chappert, Phys. Rev. B **49**, 12 888 (1994).
[3] N. Nakajima, T. Koide, T. Shidara, H. Miyauchi, H. Fukutani, A. Fujimori, K. Iio, T. Katayama, M. Nývlt, and Y. Suzuki, Phys. Rev. Lett. **81**, 5229 (1998).
[4] C. J. Tatnall, J. P. Schille, P. J. Grundy, and D. G. Lord, J. Magn. Magn. Mater. **165**, 391 (1997).
[5] H. A. Dürr, S. S. Dhesi, E. Dudzik, D. Knabben, G. van der Laan, J. B. Goedkoop, and F. U. Hillebrecht, Phys. Rev. B **59**, R701 (1999).
[6] B. N. Engel, M. H. Wiedmann, R. A. V. Leeuwen, and C. M. Falco, J. Magn. Magn. Mater. **126**, 532 (1993).
[7] T. Koide, H. Miyauchi, J. Okamoto, T. Shidara, A. Fujimori, K. Amemiya, H. Takeshita, S. Yuasa, T. Katayama, and Y. Suzuki, Phys. Rev. Lett. **87**, 257201 (2001).
[8] S. K. Kim and J. B. Kortright, Phys. Rev. Lett. **86**, 1347 (2001).
[9] F. López-Urías, J. Dorantes-Dávila, and H. Dreyssé, J. Magn. Magn. Mater. **165**, 262 (1997).
[10] L. Szunyogh, B. Újfalussy, P. Bruno, and P. Weinberger, J. Magn. Magn. Mater. **165**, 254 (1997).
[11] R. Vollmer, T. Gutjahr-Löser, J. Kirschner, S. van Dijken, and B. Poelsema, Phys. Rev. B **60**, 6277 (1999).
[12] S. van Dijken, R. Vollmer, B. Poelsema, and J. Kirschner, J. Magn. Magn. Mater. **210**, 316 (2000).
[13] B. Schulz and K. Baberschke, Phys. Rev. B **50**, 13 467 (1994).
[14] O. Robach, C. Quiros, P. Steadman, K. F. Peters, E. Lundgren, J. Alvarez, H. Isern, and S. Ferrer, Phys. Rev. B **65**, 054423 (2002).
[15] S. Hope, E. Gu, B. Choi, and J. A. C. Bland, Phys. Rev. Lett. **80**, 1750 (1998).
[16] S. Hope, E. Gu, B. Choi, and J. A. C. Bland, Phys. Rev. B **57**, 7454 (1998).
[17] H. J. Elmer, J. Hauschild, and U. Gradmann, J. Magn. Magn. Mater. **198-199**, 222 (1999).
[18] J. Chen and J. L. Erskine, Phys. Rev. Lett. **68**, 1212 (1992).
[19] R. Vollmer and J. Kirschner, Phys. Rev. B **61**, 4146 (2000).
[20] T. Yokoyama, K. Amemiya, M. Miyachi, Y. Yonamoto, D. Matsumura, and T. Ohta, Phys. Rev. B **62**, 14 191 (2000).
[21] K. Amemiya, T. Yokoyama, Y. Yonamoto, M. Miyachi, Y. Kitajima, and T. Ohta, Jpn. J. Appl. Phys., Part 2 **39**, L63 (2000).
[22] K. Amemiya, T. Yokoyama, Y. Yonamoto, D. Matsumura, and T. Ohta, Phys. Rev. B **64**, 132405 (2001).
[23] K. Christmann, O. Schober, G. Ertl, and M. Neumann, J. Chem. Phys. **60**, 4528 (1974).
[24] K. Amemiya, H. Kondoh, T. Yokoyama, and T. Ohta, J. Electron Spectrosc. Relat. Phenom. (to be published).
[25] R. Nakajima, J. Stöhr, and Y. U. Idzerda, Phys. Rev. B **59**, 6421 (1999).
[26] B. T. Thole, P. Carra, F. Sette, and G. van der Laan, Phys. Rev. Lett. **68**, 1943 (1992).
[27] P. Carra, B. T. Thole, M. Altarelli, and X. Wang, Phys. Rev. Lett. **70**, 694 (1993).
[28] O. Eriksson, B. Johansson, R. C. Albers, A. M. Boring, and M. S. S. Brooks, Phys. Rev. B **42**, 2707 (1990).
[29] W. L. O'Brien, T. Droubay, and B. P. Tonner, Phys. Rev. B **54**, 9297 (1996).
[30] S. K. Kim, Y. M. Koo, V. A. Chernov, and H. Padmore, Phys. Rev. B **53**, 11114 (1996).
[31] S. K. Kim, Y. M. Moo, V. A. Chernov, J. B. Kortright, and S. C. Shin, Phys. Rev. B **62**, 3025 (2000).
[32] J. Lahtinen, J. Vaari, and K. Kauraala, Surf. Sci. **418**, 502 (1998).
[33] Š. Pick and H. Dreyssé, Phys. Rev. B **59**, 4195 (1999).